

Green and rapid synthesis of dihydropyrimido [4,5-*b*]quinolinetrione derivatives using CoFe₂O₄@PPA as high efficient solid acidic catalyst under ultrasonic irradiation

Leila Moradi  | Pegah Mahdipour

Department of Organic Chemistry,
Faculty of Chemistry, University of
Kashan, Kashan, I. R. Iran

Correspondence

Leila Moradi, Department of Organic
Chemistry, Faculty of Chemistry,
University of Kashan, P.O. Box
8731753153, Kashan, I.R. Iran.
Email: l_moradi@kashanu.ac.ir

Funding information

Chemistry Department of University of
Kashan, Grant/Award Number: 784946

A new high efficient and green protocol for the preparation of dihydropyrimido [4,5-*b*]quinolinetrione derivatives using magnetically solid acid catalyst was presented. High performance solid acid catalyst was prepared through a three-step reaction. Firstly, CoFe₂O₄ nano particles were synthesized using co-precipitation method. In second step, CoFe₂O₄ nano particles were coated with SiO₂ shell through treatment with tetraethyl orthosilicate (CoFe₂O₄@SiO₂). Finally, CoFe₂O₄@SiO₂ was modified with polyphosphoric acid (CoFe₂O₄@SiO₂/PPA) in a simple manner. Green reusable catalyst was characterized in details using FTIR, VSM, TEM, FESEM, EDX and used as catalyst for the synthesis of dihydropyrimido[4,5-*b*]quinolinetrione derivatives. Reaction was performed under ultrasonic irradiation as green, effective and mild conditions and products were achieved in high to excellent yields. Green and eco-friendly conditions, short reaction times with high yield of products in addition to easy workup are some merits of presented method.

KEYWORDS

CoFe₂O₄@SiO₂/PPA, dihydropyrimido[4,5-*b*]quinolinetrione, green chemistry, solid acidic catalyst, ultrasonic irradiation

1 | INTRODUCTION

Now a day, sonochemistry as a new approach in organic synthesis has attracted much attention. Ultrasonic irradiation as an energy source, offers a versatile and effective route for the synthesis of a wide variety of organic compounds.^[1–10] Ultrasonic effect on molecules doesn't come from direct interaction of ultrasonic irradiation in solution.^[11,12] Instead, sonochemistry created from acoustic cavitations (the formation, growth, and implosive collapse of bubbles in a liquid). Bubble collapse made enormous amounts of energy from the conversion of the kinetic energy of the liquid motion into heating. The temperature of these bubbles is around 5000 K, with pressures of roughly 1000 atm.^[13,14] Thus, the ultrasonic irradiation provided a green, powerful,

rapid, safe, clean and efficient condition for synthetic chemistry.^[15–20]

Multi component reactions (MCRs) as an effective synthetic method have been used to the formation of carbon-carbon or carbon-heteroatom bonds through combined multiple reactions. This type of reactions offers a wide range of complex molecules in a single step. Environmentally benign, time and reagent saving, atom economy in addition to operational simplicity and reduced steps of work ups are some of the advantages of MCRs.^[21–28] In recent years, MCRs were used for the synthesis of heterocyclic compounds. Heterocycles containing pyrimidine scaffold (as a core unit) and their analogues have received considerable attentions due to their biological and pharmaceutical activities^[29–33] such as antibacterial,^[34] antileishmaniasis,^[35] antitumor^[36] and anti-

inflammatory.^[37] Furthermore, due to unique biological and pharmacological properties of pyrimido [4, 5-*b*] quinoline derivatives such as antioxidant,^[38] antitumor^[39] and antiviral^[40] activities, synthesis of this class of compounds have gained great interest in synthetic organic chemistry. Recently, various methods were published for the synthesis of pyrimido [4, 5-*b*] quinolintriones through multicomponent condensation reaction in the presence of different catalyst such as $\text{RuCl}_3 \cdot x\text{H}_2\text{O}$,^[41] tungstophosphoric acid ($\text{H}_3\text{PW}_{12}\text{O}_{40}$) under ultrasonic irradiation,^[42] TEBAC^[43] and [MSim]Cl ionic liquid.^[44] In spite of potential benefits of these methods, some of them suffer from disadvantages such as long reaction times, low yields, high temperature and the use of toxic solvents in addition to the formation of side products.

In this paper, we developed a green and efficient protocol for the synthesis of dihydropyrimido[4,5-*b*] quinolinetrione derivatives through one-pot condensation of benzaldehyde derivatives, dimedone, barbituric acid and amines in the presence of polyphosphoric acid supported on CoFe_2O_4 nanoparticles ($\text{CoFe}_2\text{O}_4@/\text{SiO}_2/\text{PPA}$) as a magnetically recoverable solid acid catalyst. The reaction was performed under ultrasonic irradiation as a powerful and green route in ambient conditions. High yield of products and short reaction times are the considerable merits of presented protocol (Scheme 1).

2 | RESULTS AND DISCUSSION

Study on the formation of CoFe_2O_4 nanoparticles was supported by FTIR spectroscopy. As can be seen in Figure 1a, the broad absorption peak in the FTIR spectra of CoFe_2O_4 nanoparticles around 3414 cm^{-1} is attributed to the normal stretching vibration of -OH groups on nanoparticle surfaces and H_2O molecules, which come from moisture in the nanocrystalline sample and adsorbed water with KBr. The weak doublet band at 2850 and 2921 cm^{-1} regions is from symmetric and anti-symmetric stretching modes of -CH group of methylene ($-\text{CH}_2-$) from remained solvents between nanoparticles. The band in 587 cm^{-1} and 1624 cm^{-1} regions are from metal-oxygen stretching vibration bonds.^[45]

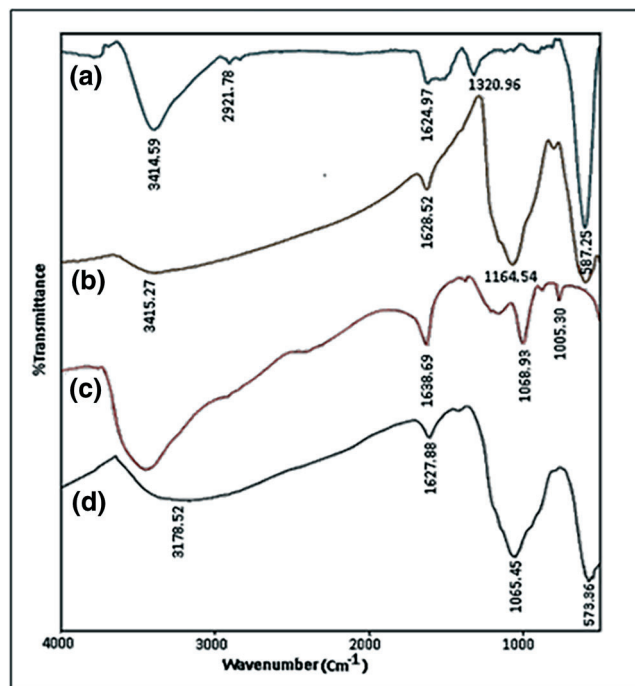
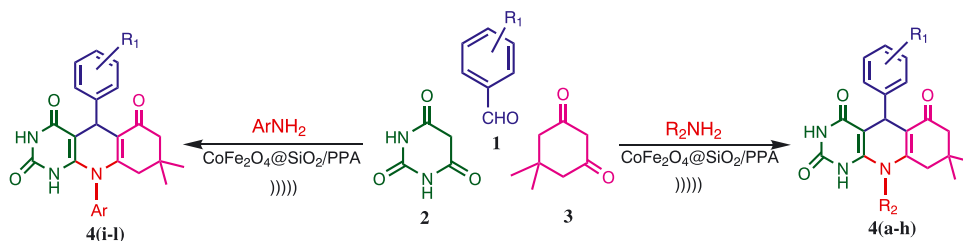


FIGURE 1 FTIR of a) CoFe_2O_4 nanoparticles, b) $\text{CoFe}_2\text{O}_4@/\text{SiO}_2$ c) PPA and d) $\text{CoFe}_2\text{O}_4@/\text{SiO}_2/\text{PPA}$

$\text{CoFe}_2\text{O}_4@/\text{SiO}_2$ exhibits strong band in 586 cm^{-1} due to metal oxide skeleton. The characteristic band of Si-O is observed at 1164 cm^{-1} and also the peak at 1628 cm^{-1} shows the existence of Fe-O vibrations. Also, the broad band at 3415 cm^{-1} is from stretching vibration of -OH groups (Figure 1b). In FTIR spectra of PPA (Figure 1c), a broad peak at about 2400 to 3400 cm^{-1} can be assigned to P-OH stretching vibrations. Peaks at 1005 and 1065 cm^{-1} regions are from stretching vibration of P-O bands; also the sign at 1638 cm^{-1} come from O groups. In FTIR spectra of $\text{CoFe}_2\text{O}_4@/\text{SiO}_2/\text{PPA}$ (Figure 1d), the main peaks of Si-O and PPA are existed and confirmed the chemically attachment of PPA (through TEOS as linker) to nanoparticle surfaces.

XRD pattern of as prepared and modified CoFe_2O_4 are presented in Figure 2. As can be seen, the XRD patterns show the reflections namely (220), (311), (222), (400), (422), (511) and (440) that are indexed based on the JCPDS standard. All peaks are in agreement with the



SCHEME 1 Synthesis of dihydropyrimido[4,5-*b*]quinolinetriones using $\text{CoFe}_2\text{O}_4@/\text{SiO}_2/\text{PPA}$ under ultrasonic irradiation

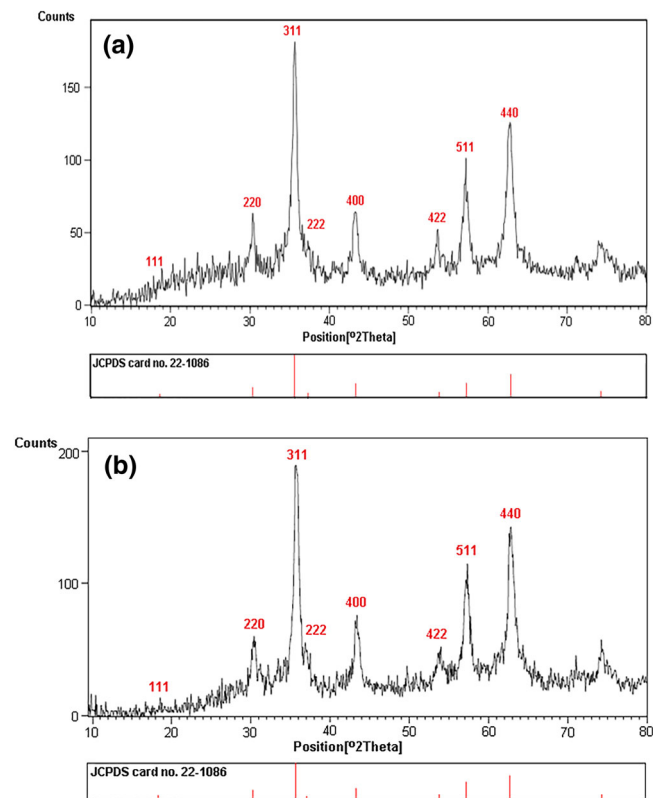


FIGURE 2 XRD pattern of: CoFe₂O₄ nanoparticles (a) and CoFe₂O₄@SiO₂/PPA (b)

single-phase spinel structure. The average crystal size of CoFe₂O₄ nanoparticles was about 28 nm (calculated by Scherrer equation).^[46] On the other hand, the XRD

pattern of modified nanoparticles is as the same of pristine nanoparticles and demonstrates that modification process had no damaging effect on crystallinity of CoFe₂O₄ structure.

Further characterization of raw and modified nanoparticles was done using FESM technique (Figure 3). It is clear that the dually metal oxide nanoparticles were prepared in nanoscale with size of about 22 to 27 nm and good distribution. Also, FESEM image of treated nanoparticles (CoFe₂O₄@SiO₂/PPA) show that the size of nanoparticles becomes larger than raw material due to surface modification and also no changes and damaging occurred on nanoparticles structure. TEM images of catalyst (Figure 3c, 3d), demonstrated the nanometric size and good dispersion of nano catalyst particles. Obtain results from FESEM and TEM techniques are in good agreement with those concluded from the XRD analysis (Figure 2).

The EDX spectra display the composition of as prepared and modified CoFe₂O₄ nanoparticles. As can be seen in Figure 4a, pristine CoFe₂O₄ nanoparticles are contained to Fe, O and Co elements. In the EDX spectrum of CoFe₂O₄@SiO₂/PPA (Figure 4b), Si and P were observed in addition to Fe, Co and O elements. The presence of Si and P in composition of prepared catalyst (13 and 10% respectively), demonstrated the attachment of SiO₂/PPA on nanoparticle surfaces.

Thermogravimetric analysis was used to confirm the attachment of SiO₂/PPA groups on CoFe₂O₄ nanoparticles surfaces (Figure 5). Figure 5a shows that there is no

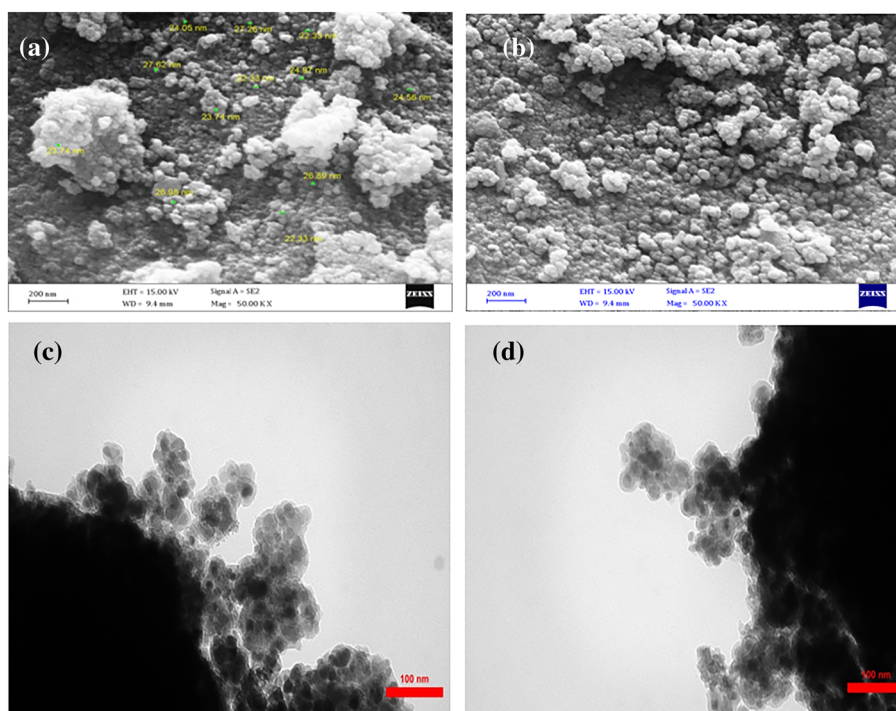


FIGURE 3 FESEM images of: a) CoFe₂O₄ and b) CoFe₂O₄@SiO₂/PPA and TEM images of CoFe₂O₄@SiO₂/PPA (C,d)

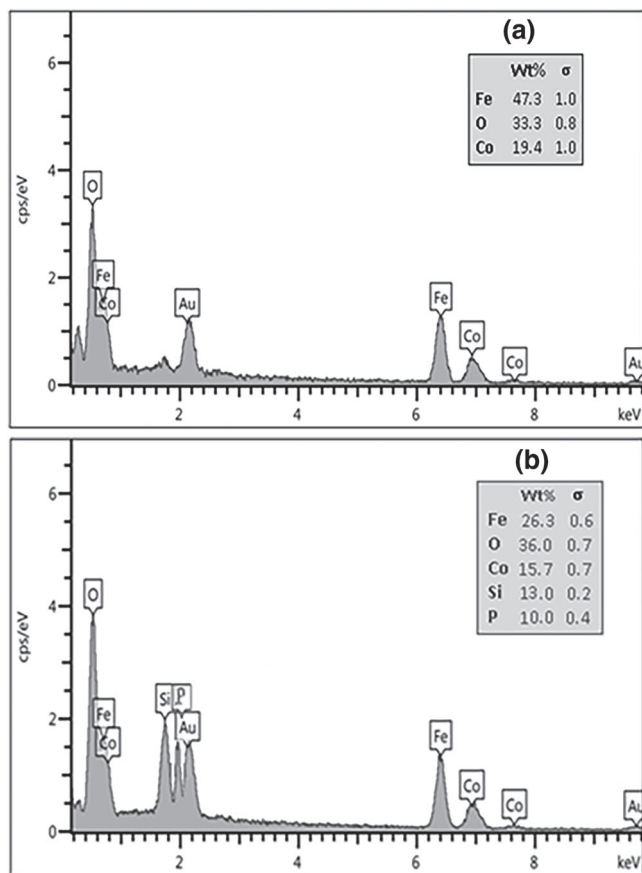


FIGURE 4 EDX spectra of a: CoFe₂O₄ and b: CoFe₂O₄@SiO₂/PPA

weight loss in TGA curve of CoFe₂O₄ nanoparticles. Instead, TGA analysis of catalyst shows a weight loss of 3% at the range of 50 to 150 °C which is related to the removal of water that physically adsorbed on nanoparticle surfaces. The weight loss of about 19% between 150 to 600 °C is attributed to the thermal decomposition of PPA and linker (TEOS) that were chemically attached on nanoparticle surfaces (Figure 5b). Results from TGA curves confirmed the immobilization of SiO₂/PPA groups to the CoFe₂O₄ nanoparticle surfaces.

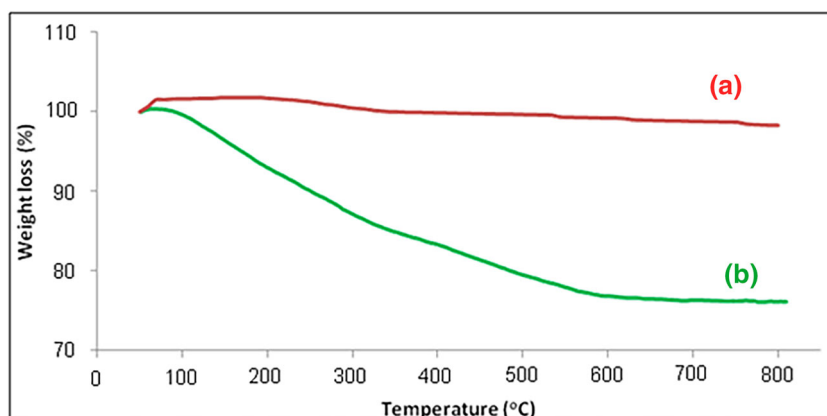


FIGURE 5 TGA curves of a: CoFe₂O₄ and b: CoFe₂O₄@SiO₂/PPA

Magnetic characterization of CoFe₂O₄ nanoparticles and CoFe₂O₄@SiO₂/PPA was done using vibrating sample magnetometer (VSM) at room temperature with maximum applied field of 15 kOe (Figure 6). For CoFe₂O₄@SiO₂/PPA, the saturation magnetization (M_S) was 20 emu/g, while in case of CoFe₂O₄ nanoparticles the value for the same parameter was 68 emu/g. This result is attributed to the effect of modification which subsequently decreases the saturation magnetization

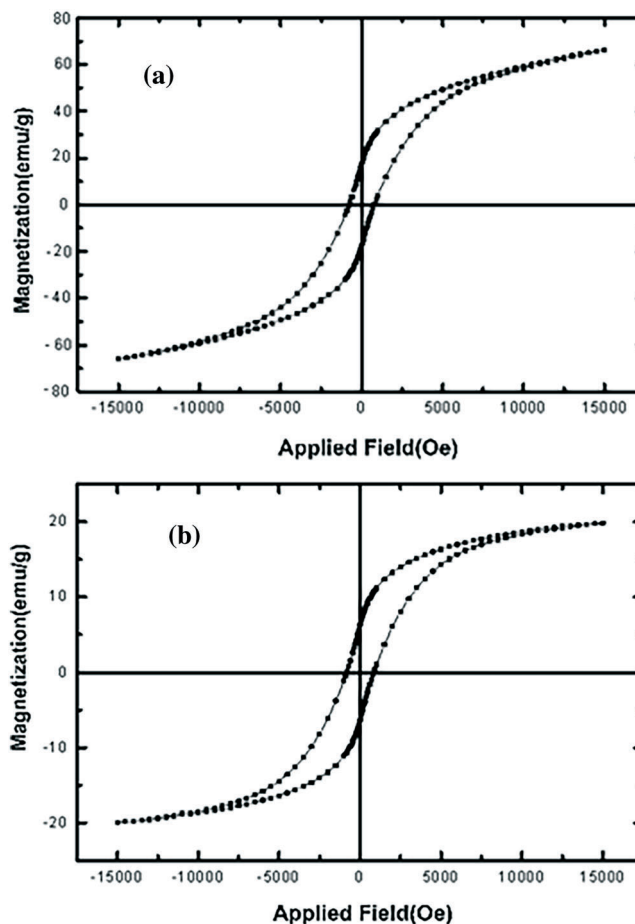


FIGURE 6 VSM analysis of: a) CoFe₂O₄ nanoparticles and b) CoFe₂O₄@SiO₂/PPA

value. Consequently, synthesis of catalyst has been occurred successfully.

In continue of our research, the prepared and characterized catalyst was applied for multicomponent preparation of dihydropyrimido[4,5-*b*]quinolinetriene derivatives under ultrasonic irradiation. Firstly, the best amount of catalyst was estimated using the four component reaction of aniline, barbituric acid, dimedone and benzaldehyde (as model reaction) in EtOH. Several tests were done in the presence of various amounts of catalyst under ultrasonic irradiation with the power of 50 w. As can be seen in Table 1, 0.01 g of catalyst was the best quantity to achieve the product in the highest yield (95% entry 4). Also, the further amount of catalyst has any effect on the yield of product.

After determining the best amount of catalyst, solvent effect on the time and yield of reaction was studied. Model reaction was done in the presence of 0.01 g of catalyst under ultrasonic irradiation (with power of 50 w) in different solvent media. Results depicted in Table 2 shows that EtOH can be considered as suited solvent (entry 4).

The influence of various power of ultrasonic irradiation on reaction has been investigated using the performance of model reaction under ultrasonic irradiation with different powers (Table 3). It was observed that the power of 50 w was afforded the best result (entry 3). Also In order to determine the ultrasound irradiation effect on the performance of model reaction, one test was done under silent condition with magnetic stirring at room temperature (entry 5). Result shows the low yield of the desired product (after 30 min) and consequently proved the strong effect of ultrasonic waves on time, yield and performance of reaction.

The efficiency of catalyst in the presence of optimized solvent and ultrasonic power was investigated

TABLE 2 Optimization of solvent for preparation of compound **4a**

Entry	Solvent	Time (min)	Yield (%) ^a
1	CHCl ₃	10	27
2	CH ₃ CN	8	35
3	H ₂ O	9	46
4	C ₂ H ₅ OH	4	95
5	C ₂ H ₅ OH/H ₂ O	5	88

^aIsolated yield.

TABLE 3 Optimization of the power of ultrasonic irradiation for synthesis of **4a**

Entry	Power (w)	Time (min.)	Yield (%) ^a
1	30	6	83
2	40	5	85
3	50	4	95
4	60	4	92
5	-	30	21 ^b

^aIsolated yield

^bIsolated yield under silent conditions

through the preparation of dihydropyrimido[4,5-*b*]quinolinetrienes using various aniline and aldehyde derivatives. Results were collected in Table 4. As can be seen, in all cases, products were obtained in excellent yields and short reaction times. Also when terephthalaldehyde was used, the reaction time was increased to 10 min due to two aldehyde sites (4e). On the other hand, in the case of aliphatic amines and ammonium acetate (as NH₃ source), no enhancement of reaction times was observed (4i-4 l).

TABLE 1 Optimization of the catalyst amount^a

Entry	Catalyst (g)	Time (min.)	Yield (%) ^b
1	-	10	12
2	0.001	8	48
3	0.005	6	65
4	0.01	4	95
5	0.015	4	95

^aaniline (1 mmol), barbituric acid (1 mmol), dimedone (1 mmol) and benzaldehyde (1 mmol), EtOH (5 ml) under ultrasonic irradiation with power of 50 w.

^bIsolated yield.

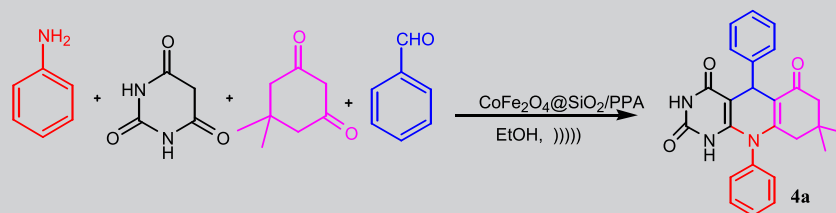
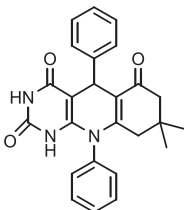
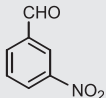
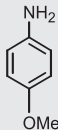
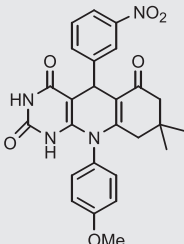
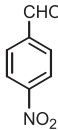
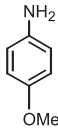
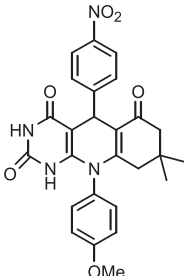
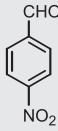
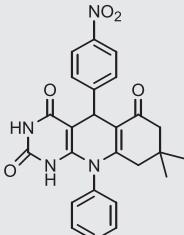
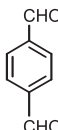
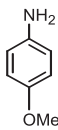
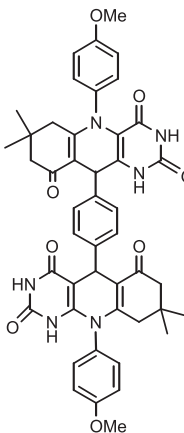


TABLE 4 Synthesis of dihydropyrimido[4,5-*b*]quinolinetriones using $\text{CoFe}_2\text{O}_4@\text{SiO}_2/\text{PPA}$

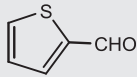
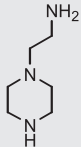
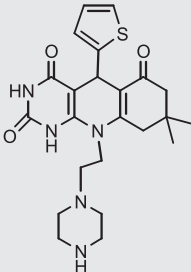
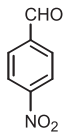
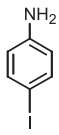
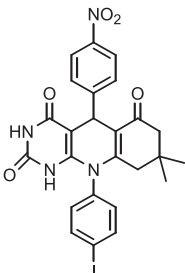
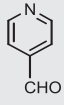
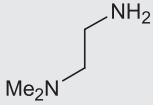
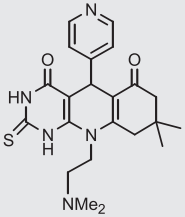
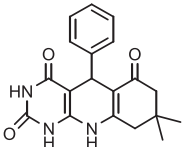
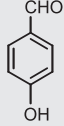
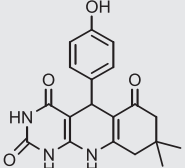
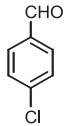
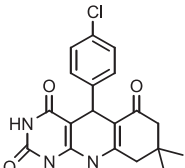
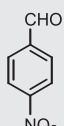
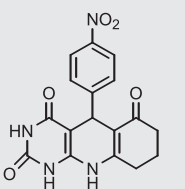
product	Aldehyde	Amine	Product	Time (min)	Yield (%)	m.p (°C)	Ref.
4a				4	95	230–232	[42]
4b				4	96	257–259	[42]
4c				3	95	253–255	-
4d				3	92	250–252	-
4e				10	92	>300	[42]

(Continues)

The efficiency of catalyst was studied through the comparison of the time and yield of reaction in the presence of other catalysts (under thermal and ultrasonic conditions). Results in Table 5 show that $\text{CoFe}_2\text{O}_4@\text{SiO}_2/\text{PPA}$ had the highest efficiency both in thermal and ultrasonic conditions (entry 11, 12).

The role of catalyst during the reaction process displays in scheme 3. According to the Khalafi-Nejhad *et al.* proposed reaction mechanism,^[42] initially, barbituric acid reacted with activated aldehyde through a Knoevenagel condensation to generate of intermediate **A**. then, dimedone (in the enol form) added to **A** in a conjugate

TABLE 4 (Continued)

product	Aldehyde	Amine	Product	Time (min)	Yield (%)	m.p (°C)	Ref.
4f				3	95	218–220	[42]
4 g				3	93	281–283	[42]
4 h				5	91	225–227	[42]
4i		CH ₃ CO ₂ NH ₄		4	90	210–212	[42]
4j		CH ₃ CO ₂ NH ₄		5	94	>300	[43]
4 k		CH ₃ CO ₂ NH ₄		4	88	>300	[47]
4l ^a		CH ₃ CO ₂ NH ₄		3	92	>300	[43]

^a1,3-cyclohexadione was used instead of dimedone

TABLE 5 Comparison the efficiency of catalysts for the synthesis of **4a**

Entry	Catalyst/condition	Time	Yield (%) ^a
1	s-NFC ^b /Ethanol, reflux	45 min	92
2	s-BC ^c /Ethanol, reflux	40 min	94
3	none/EtOH, US	10 min	16
4	none/EtOH, 80 °C	24 h	12
5 ^d	AlCl ₃ /EtOH, 80 °C	12 h	35
6	CoFe ₂ O ₄ NPs/EtOH, 80 °C	3 h	47
7	CoFe ₂ O ₄ NPs/EtOH, US	9 min	65
8	PPA/EtOH, 80 °C	7 h	70
9	PPA/EtOH, US	6 min	80
10 ^d	PTSA/EtOH, 80 °C	5 h	81
11	CoFe ₂ O ₄ @SiO ₂ /PPA/EtOH, 80 °C	4 h	90
12	CoFe ₂ O ₄ @SiO ₂ /PPA/EtOH, US	4 min	95
13	CoFe ₂ O ₄ @SiO ₂ /SO ₃ H/EtOH, 80 °C	5 h	88
14	CoFe ₂ O ₄ @SiO ₂ /SO ₃ H/EtOH, US	7 min	72
15 ^b	H ₃ PW ₁₂ O ₄₀ /EtOH, 80 °C	5 h	91

^aIsolated yield^bNanofibrillated cellulose sulfuric acid^[48]^cNanobacterial cellulose sulfuric acid^[48]

Reference 39

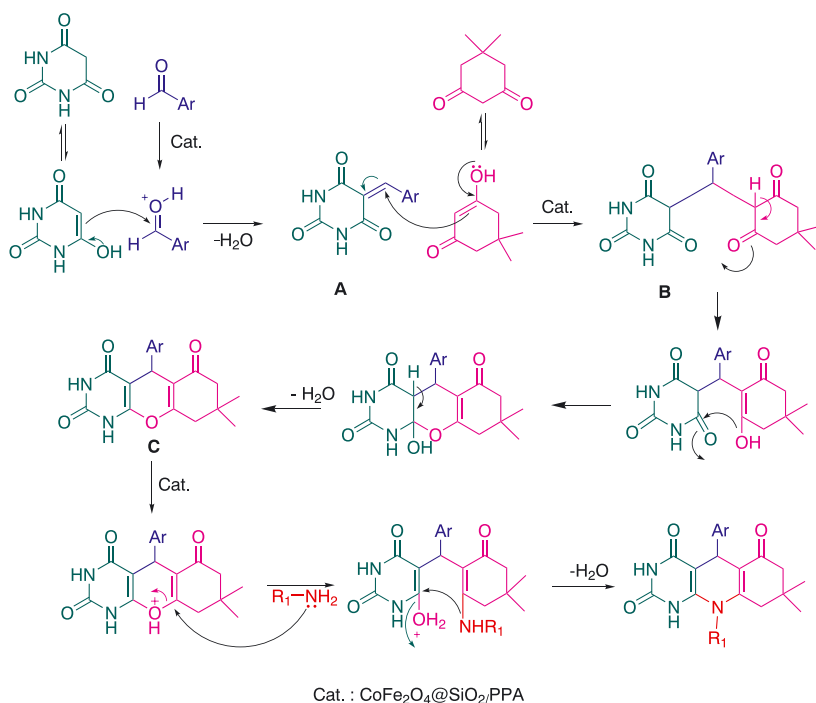
route to produced intermediate **B**. after the intramolecular condensation of **B**, and then water removal, **C** is formed. In continue, the reaction of amine with **C** and

water elimination, lead to the desired product (Scheme 2).

Further evidence for demonstrating the proposed mechanism was the separation and characterization of intermediate **C** (8,8-Dimethyl-5-phenyl-8,9-dihydro-1*H*-chromeno[2,3-*d*]pyrimidine-2,4,6(3*H*,5*H*,7*H*)-trione) that generates from the reaction of barbituric acid, arylaldehyde and dimedone in the presence of catalyst. Spectral data from FTIR and ¹HNMR analysis of **C** was shown that mentioned intermediate was made through the reaction process and the reaction was proceeded according to mechanism which presented in Scheme 2.

Reusability of catalyst was examined using model reaction under optimized conditions. As shown in Figure 7a, the catalyst can be easily separated from the reaction mixture by an external magnet. After completion of the reaction, catalyst was separated and washed with ethanol (twice) and dried at 80 °C for 4 h. The dried catalyst was reused six times for the same reaction. As can be seen in Figure 7b, the catalyst has good efficiency after six times recycling with low decreasing in yield of product. Figure 8 shows the SEM photograph of reused catalyst. As can be seen, there are no changes in morphology of nanocatalyst after recycling and this result is consistent with FTIR and XRD pattern of recycled sample (Figure 9).

In order to verify the stability of catalyst during the reaction process, hot filtration method was carried out. In this way, the catalytic synthesis of compound **4a** was carried out under ultrasonic irradiation. The reaction was performed for 2.5 min and then the catalyst was

**SCHEME 2** Reaction mechanism for the preparation of dihydropyrimido[4,5-*b*]quinolinetriones using CoFe₂O₄@SiO₂/PPA

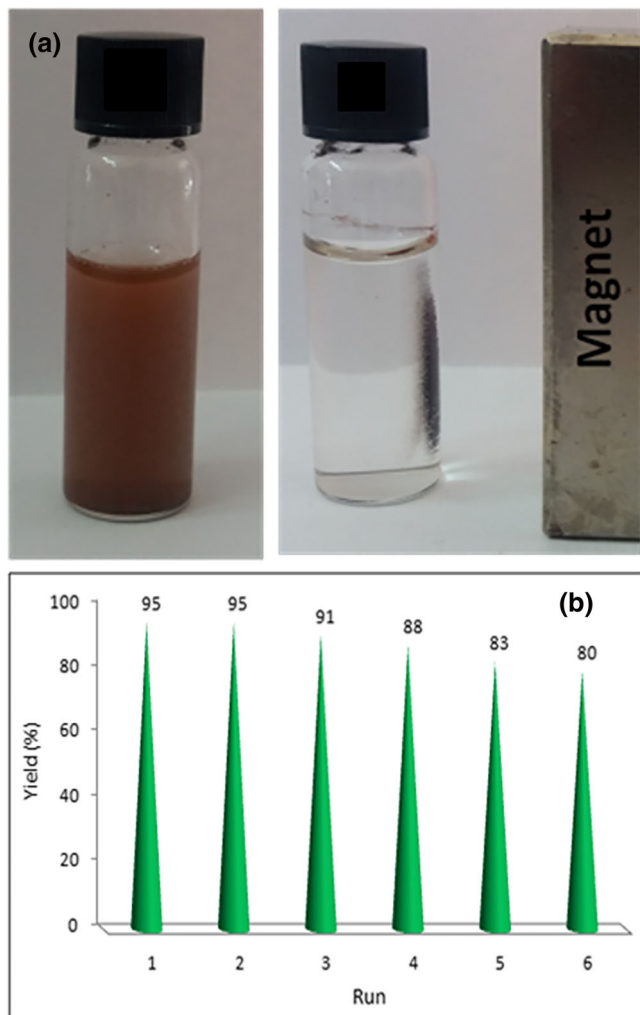


FIGURE 7 Separation of magnetically catalyst by external magnet (a), reusability of $\text{CoFe}_2\text{O}_4@\text{SiO}_2/\text{PPA}$ (b)

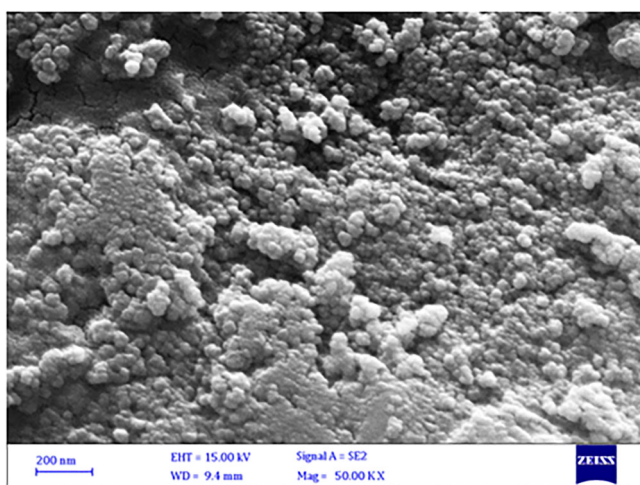


FIGURE 8 SEM image of recycled catalyst

separated using external magnetic field. After that, reaction mixture (without $\text{CoFe}_2\text{O}_4@\text{SiO}_2/\text{PPA}$) was continued for other 1.5 min. as can be seen in Figure 10, the

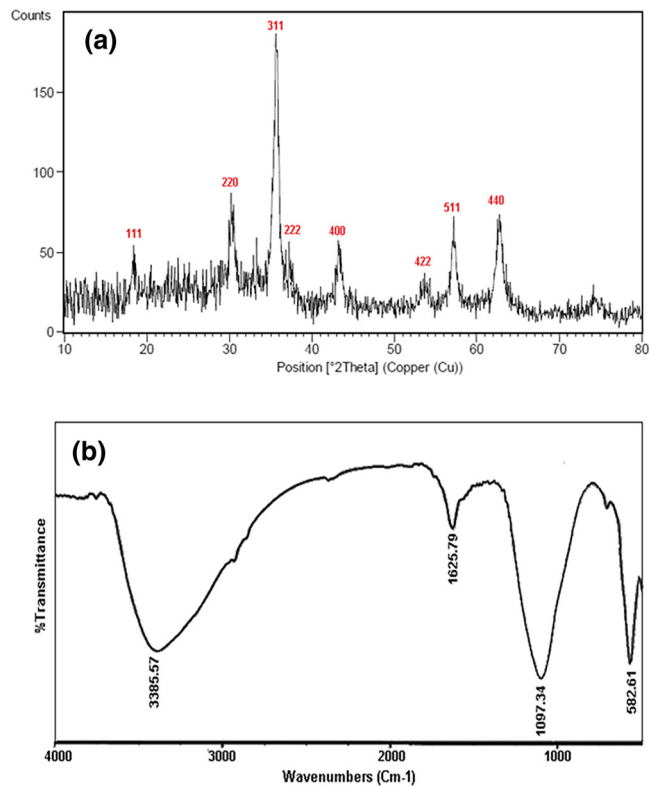


FIGURE 9 XRD pattern (a) and FTIR (b) of recycled catalyst

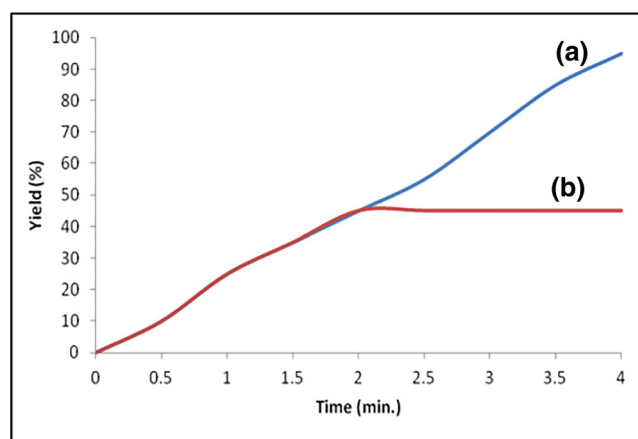


FIGURE 10 Hot filtration result for the synthesis of dihydropyrimido [4,5-b]quinolinetrione derivatives without catalyst filtration (blue diagram) and catalyst filtration after 2 min (red diagram)

yield of product was stable after removal of catalyst and obtained result proved that $\text{CoFe}_2\text{O}_4@\text{SiO}_2/\text{PPA}$ is stable during the reaction and *no catalyst leaching was observed*.

To continue, ICP-AES analysis was carried out for CoFe_2O_4 , $\text{CoFe}_2\text{O}_4@\text{SiO}_2/\text{PPA}$ and recycled catalyst. According to results depicted in Table 6, the content of Co and Fe was 19.8 and 46.4% in CoFe_2O_4 nanoparticles that was in agreement with EDX result. The weight percentage of Co and Fe in the fresh catalyst

TABLE 6 BET and ICP analysis of CoFe₂O₄, CoFe₂O₄@SiO₂/PPA and recovered catalyst

Sample	BET (m ² /g)	ICP	
		%Co	%Fe
CoFe ₂ O ₄	110.2	19.8	46.4
CoFe ₂ O ₄ @SiO ₂ /PPA	82.1	16.5	23.6
CoFe ₂ O ₄ @SiO ₂ /PPA after 1st use	79.6	16.2	23.1

(CoFe₂O₄@SiO₂/PPA) was 16.5 and 23.6% respectively also the content of Co and Fe in the recovered catalyst was 16.2 and 23.1 wt%. Based on these results, it can be concluded that there is no substantial difference in weight percentage of Co and Fe in fresh and recovered catalyst and subsequently, no leaching occurred.

The surface area of CoFe₂O₄ nanoparticles, fresh and recycled catalyst was determined by the nitrogen physical adsorption and was carried out at liquid nitrogen boiling point. The surface area of CoFe₂O₄ nanoparticles and CoFe₂O₄@SiO₂/PPA was 110.5 and 82.1 m² g⁻¹, respectively (Table 6). The lower surface area of catalyst is a consequence of successful immobilizing the polyphosphoric acid onto the surfaces of silica coated CoFe₂O₄ nanoparticles. Also the surface area of the first recycled catalyst was 79.6 m² g⁻¹ that shows the surface area of recycled catalyst was close to the fresh sample and no considerable poisoning happened on the catalyst surfaces.

3 | EXPERIMENTAL

3.1 | Materials and methods

Chemical reagents were purchased from the Merck and Aldrich Company. Melting points were determined in open capillaries using an Electro thermal MK3 apparatus. FTIR spectra were recorded using a Perkin-Elmer FT-IR 550 Spectrometer. ¹H NMR and ¹³CNMR spectra were recorded with a Bruker Avance DPX-400 spectrometer at 400 and 100 MHz, respectively. Magnetic properties were characterized by a vibrating sample magnetometer (VSM, MDKFD) at room temperature. FE-SEM images and EDX analysis were used by a Sigma ZEISS, Oxford Instruments Field Emission Scanning Electron Microscope. Ultrasonication was performed in a BANDELIN ultrasonic HD 3200 instrument with probe model US 70/T with diameter of 6 mm that was immersed directly into the reaction mixture. The operating frequency was 20 KHz and the output power was 30–60 W through manual adjustment. Mass spectroscopic analysis was recorded on a Finnigan MAT 44S by Electron Ionization (EI) mode with an ionization voltage of 70 eV. Elemental analyses of the

catalyst with inductively coupled plasma optical emission spectroscopy (ICP-AES) were obtained from an ICP-AES simultaneous instrument (VISTA-PRO). Brunauer Emmett Teller (BET) analysis was used to determine the surface area of catalyst by Microtrac BEL Corp instrument. All of characterisation data for prepared catalyst were cited in results and discussion section and also the analysis data of synthesized products will cited in experimental section (Supporting Information).

3.2 | Preparation of CoFe₂O₄ nanoparticles

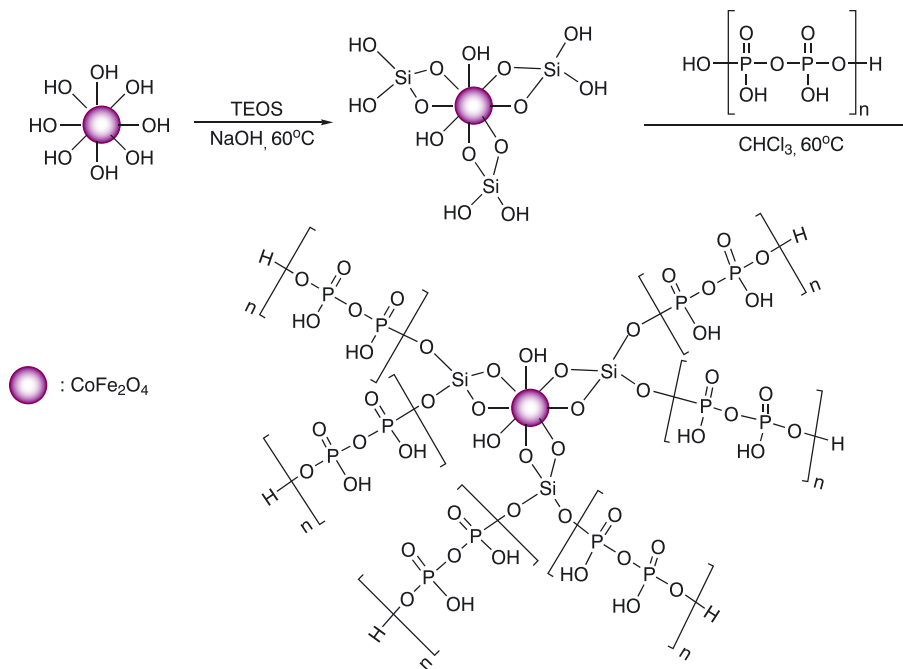
A mixture of FeCl₃·6H₂O (0.54 g, 2 mmol) and CoCl₂·6H₂O (0.13 g, 1 mmol) dissolved in distilled water ((100 ml) was poured to a three-necked flask equipped with a mechanical stirrer. Then, a solution of NaOH (3 mol/L, 50 ml) was added and stirred vigorously for 20 min. After that, the mixture was heated to reflux for 2 hr to yield a black dispersed mixture. Then, nanoparticles were separated with an external magnet and washed with distilled water and ethanol for three times to reach the neutral PH and finally dried at 100 °C for 24 hr.

3.3 | Preparation of CoFe₂O₄@SiO₂/PPA

In order to prepare of the catalyst, firstly, CoFe₂O₄ nanoparticles were coated with silica layer. A dispersed solution of CoFe₂O₄ nanoparticles (1 g in 50 ml EtOH) was prepared using sonication in a bath sonicator for 30 min. Then, a concentrated ammonia solution (2 ml) was added and stirred for 30 min at 60 °C. After that, tetraethylorthosilicate (TEOS) (1.0 ml dissolved in 10 ml EtOH) was added drop wise to the reaction mixture and continuously stirred at 60 °C for 24 hr. After the time, the silica coated nanoparticles (CoFe₂O₄@SiO₂) were separated using an external magnetic field and washed with methanol (three times) and dried. For preparing the CoFe₂O₄@SiO₂/PPA, polyphosphoric acid (0.5 g) dissolved in CHCl₃ (50 ml) was poured in a round-bottom flask and stirred at 50 °C for 2 hr; then, CoFe₂O₄@SiO₂ (1 g) was added and stirred for 4 hr. After that, resulted solid was separated and washed with cold absolute EtOH and dried in vacuo at 80 °C (Scheme 3). The amount of H⁺ determined by acid–base titration was about 0.7 mmol/g.

3.4 | General procedure for preparation of dihydropyrimido[4,5-*b*]quinolinetriene derivatives

A mixture of barbituric acid (1 mmol), dimedone (1 mmol), aromatic aldehyde (1 mmol), and CoFe₂O₄@SiO₂/PPA



SCHEME 3 Preparation process of CoFe₂O₄@SiO₂/PPA

(0.01 g) in EtOH (5 ml) was sonicated (by probic sonicator) for 1 min with power of 50 w; after that, amine (1 mmol) was added and sonicated under the same power. The progress of the reaction was monitored by TLC. After the completion of the reaction, the mixture was cooled to room temperature and 5 ml EtOH was added and the catalyst was separated using an external magnet. Obtained product was separated using simple filtration and washed with EtOH and *n*-hexane to afford the pure products.

3.4.1 | Spectral data

8,8-Dimethyl-5,10-diphenyl-8,9-dihydropyrimido[4,5-*b*]quinoline-2,4,6(1*H*,3*H*,5*H*,7*H*,10*H*)-trione (4a)

Yield: 95%; pale yellow solid; mp 230–232 °C; FTIR (KBr) $\bar{\nu}$ (cm⁻¹): 3200 (NH), 3000 (C=C-H), 2923 (C-H), 1692 (C=O), 1493 (C=C aromatic); ¹H NMR (DMSO-*d*₆, 400 MHz): δ (ppm) 0.93 (s, 3H, CH₃), 1.30 (s, 3H, CH₃), 2.29–2.49 (m, 4H, 2CH₂), 5.98 (s, 1H, CH), 6.73 (d, 2H, *J* = 8 Hz, H-Ar), 6.98–7.16 (m, 6H, H-Ar), 10.30 (s, 1H, NH), 10.90 (s, 1H, NH); Anal. Calcd for C₂₅H₂₃N₃O₃ (413.47): C, 72.62; H, 5.61; N, 10.16; O, 11.61; Found: C, 72.58; H, 5.59; N, 10.13; O, 11.58.

10-(4-Methoxyphenyl)-8,8-dimethyl-5-(3-nitrophenyl)-8,9-dihydropyrimido[4,5-*b*]quinoline-2,4,6(1*H*,3*H*,5*H*,7*H*,10*H*)-tri- one (4b)

Yield: 96%; yellow color; mp 257–259 °C, FTIR (KBr) $\bar{\nu}$ (cm⁻¹): 3200 (NH), 2956 (C-H), 1692 (C=O), 1596 (C=C aromatic), 1344 (NO₂); ¹H NMR (DMSO-*d*₆, 400 MHz) δ

(ppm): 1.02 (s, 6H, 2CH₃), 2.18–2.39 (m, 4H, 2CH₂), 3.37 (s, 3H, CH₃), 6.15 (s, 1H, CH), 6.95 (d, 2H, *J* = 8 Hz, H-Ar), 7.14 (d, 2H, *J* = 8 Hz, H-Ar), 7.46 (d, *J* = 8 Hz, 2H, H-Ar), 7.80 (s, 1H, H-Ar), 7.88–7.92 (m, 1H, H-Ar), 9.71 (s, 1H, NH), 10.22 (s, 1H, NH); Anal. Calcd for C₂₆H₂₄N₄O₆ (488.49): C, 63.93; H, 4.95; N, 11.47; O, 19.65; Found: C, 63.90; H, 4.91; N, 11.43; O, 19.59.

10-(4-methoxyphenyl)-8,8-dimethyl-5-(4-nitrophenyl)-5,8,9,10-tetrahydropyrimido[4,5-*b*]quinoline-2,4,6(1*H*,3*H*,7*H*)-trione (4c)

Yield: 95%; white solid; mp 253–252 °C; FTIR (KBr) $\bar{\nu}$ (cm⁻¹): 3100 (NH), 3031 (C=C-H), 2984 (C-H), 1688 (C=O), 1601 (C=C aromatic), 1154 (C-O); ¹H NMR (DMSO-*d*₆, 400 MHz): δ (ppm) 0.91 (s, 6H, 2CH₃), 2.00–2.31 (m, 4H, 2CH₂), 3.72 (s, 3H, CH₃), 6.12 (s, 1H, CH), 6.93 (d, 2H, *J* = 8 Hz, H-Ar), 7.12 (d, 2H, *J* = 8 Hz, H-Ar), 7.65 (d, 2H, *J* = 8 Hz, H-Ar), 7.79–7.97 (m, 4H, Ar-H), 9.81 (s, 1H, NH), 10.22 (s, 1H, NH); ¹³C NMR (DMSO-*d*₆, 75 MHz): δ (ppm) 27.30, 30.20, 31.40, 56.20, 88.35, 90.50, 119.15, 120.25, 122.50, 124.40, 127.35, 128.20, 130.10, 148.60, 149.30, 152.30, 153.40, 155.50, 164.10; Anal. Calcd for C₂₆H₂₄N₄O₆ (488.49): C, 63.93; H, 4.95; N, 11.47; O, 19.65; Found: C, 63.90; H, 4.91; N, 11.43; O, 19.59.

8,8-dimethyl-5-(4-nitrophenyl)-10-phenyl-5,8,9,10-tetrahydropyrimido[4,5-*b*]quinoline-2,4,6(1*H*,3*H*,7*H*)-trione (4d)

Yield: 92%; white solid; mp 250–252 °C; FTIR (KBr) $\bar{\nu}$ (cm⁻¹): 3336 (NH), 3023 (C=C-H), 1692 (C=O), 1616 (C=C aromatic), 1406 (NO₂); ¹H NMR (DMSO-*d*₆,

400 MHz): δ (ppm) 1.01(s, 6H, 2CH₃), 2.06 (s, 4H, 2CH₂), 6.11 (s, 1H), 6.91–7.95 (m, 3H, H-Ar), 7.25 (d, 4H, $J = 8$ Hz, H-Ar), 8.04–8.21 (m, 2H, H-Ar), 10.12 (s, 1H, NH), 10.91 (s, 1H, NH); Anal. Calcd for C₂₅H₂₂N₄O₅ (458): C, 65.50; H, 4.80; N, 17.46; O, 12.24, Found: C, 65.51; H, 4.78; N, 17.42; O, 12.29; MS (ESI) m/z : 458 (M⁺), 256 (55), 226 (100), 128 (30), 93 (90), 55 (17).

1,4-Bis[10-(4-methoxyphenyl)-8,8-dimethyl-8,9-dihydropyrimido[4,5-*b*]quinoline-2,4,6(1H,3H,5H,7H,10H)-trione]benzene (4e)

Yield: 92%; yellow solid; >300 °C; FTIR (KBr) $\bar{\nu}$ (cm⁻¹): 3078 (NH), 2959 (C=C-H), 1703 (C=O), 1568 (C=C aromatic); ¹H NMR (DMSO-d₆, 400 MHz): δ (ppm) 1.00 (s, 6H, CH₃), 2.06–2.25 (m, 4H, CH₂), 3.33 (s, 3H, OCH₃), 5.91 (s, 1H, CH), 6.90–7.12 (m, 6H, H-Ar), 9.48(s, 1H, NH), 10.06 (s, 1H, NH); Anal. Calcd for C₄₆H₄₄N₆O₈ (808.88): C, 68.30; H, 5.48; N, 10.39; O, 15.83, Found: C, 68.25; H, 5.44; N, 10.36; O, 15.95.

8,8-Dimethyl-10-[2-(piperazin-1-yl)ethyl]-5-(thiophen-2-yl)-8,9-dihydropyrimido[4,5-*b*]quinoline-2,4,6(1H,3H,5H,7H,10H)-trione (4f)

Yield: 95%; yellow color; mp 218–220 °C; FTIR (KBr) $\bar{\nu}$ (cm⁻¹): 3200 (NH), 2963 (C=C-H), 1688 (C=O), 1596 (C=C aromatic); ¹H NMR (DMSO-d₆, 400 MHz) δ (ppm): 0.93 (s, 3H, CH₃), 1.00 (s, 3H, CH₃), 1.91 (s, 1H, NH), 2.23 (m, 4H, 2CH₂), 2.48 (m, 8H, 4CH₂), 2.81 (s, 2H, CH₂), 2.95 (s, 2H, CH₂), 6.12 (s, 1H, CH), 6.31–6.54 (m, 1H, Ar-H), 6.62–6.81 (m, 1H, Ar-H), 6.92–7.12 (m, 1H, Ar-H), 9.52 (s, 1H, NH), 10.00(s, 1H, NH); Anal. Calcd for C₂₃H₂₉N₅O₃S (455.57): C, 60.64; H, 6.42; N, 15.37; O, 10.54, Found: C, 60.61; H, 6.38; N, 15.32, 10.51.

10-(4-Iodophenyl)-8,8-dimethyl-5-(4-nitrophenyl)-8,9-dihydro-pyrimido[4,5-*b*]quinoline-2,4,6(1H,3H,5H,7H,10H)-trione (4 g)

Yield: 93%; yellow solid; mp 281–283 °C; FTIR (KBr) $\bar{\nu}$ (cm⁻¹): 3336 (NH), 3100 (C=C-H), 1691 (C=O), 1599 (C=C aromatic); ¹H NMR (DMSO-d₆, 400 MHz): δ (ppm) 0.93 (s, 3H, CH₃), 1.03 (s, 3H, CH₃), 2.16–2.31 (m, 4H, 2CH₂), 5.92 (s, 1H, CH), 6.85–6.87 (d, 2H, $J = 8$ Hz, H-Ar), 7.00–7.02 (d, 2H, $J = 8$ Hz, H-Ar), 7.20–7.28 (m, 4H, Ar-H), 10.06 (s, 1H, NH), 10.85 (s, 1H, NH); Anal. Calcd for C₂₅H₂₁I_N₄O₅ (584.36): C, 51.38; H, 3.62; N, 9.59; O, 13.69, Found: C, 51.35; H, 3.59; N, 9.57; O, 13.72.

10-[2-(Dimethylamino)ethyl]-8,8-dimethyl-5-(pyridin-4-yl)-2-thioxo-2,3,8,9 tetrahydropyrimido[4,5-*b*]quinoline-4,6(1H,5H,7H,10H)-dione (4 h)

Yield: 91%; pale yellow solid; mp 225–227 °C; FTIR (KBr) $\bar{\nu}$ (cm⁻¹): 3355 (NH), 3159 (C=C-H), 1716

(C=O), 1630 (C=C aromatic); ¹H NMR (DMSO-d₆, 400 MHz) δ (ppm): 0.92 (s, 3H, CH₃), 1.00 (s, 3H, CH₃), 2.00–2.40- (m, 4H, 2CH₂), 2.52 (m, 4H, 2CH₂), 2.64 (s, 3H, NMe₂), 2.81 (s, 3H, NMe₂) 5.90 (s, 1H, CH), 6.21 (s, 1H, CH), 6.45 (d, 1H, $J = 8$ Hz, Ar-H), 6.63 (d, 1H, $J = 8$ Hz, Ar-H), 6.90–7.40 (m, 4H, Ar-H), 10.01(s, 1H, NH), 10.90 (s, 1H, NH); Anal. Calcd for C₂₂H₂₇N₅O₂S (425.55): C, 62.09; H, 6.40; N, 16.46; O, 7.52 Found: C, 62.06; H, 6.38; N, 16.45; O, 7.49.

8,8-Dimethyl-5-phenyl-8,9-dihydropyrimido[4,5-*b*]quinoline-2,4,6(1H,3H,5H,7H,10H)-trione (4i)

Yield: 90%; white solid; mp 210–212 °C; FTIR (KBr) $\bar{\nu}$ (cm⁻¹): 3200 (NH), 2954 (C=C-H), 1701 (C=O), 1584 (C=C aromatic); ¹H NMR (DMSO-d₆, 400 MHz) δ (ppm): 0.91 (s, 6H, 2CH₃), 2.00–2.31 (m, 4H, 2CH₂), 6.01 (s, 1H), 6.91–7.32 (m, 5H, H-Ar), 9.51 (s, 1H, NH), 1.00 (s, 1H, NH); Anal. Calcd for C₁₉H₁₉N₃O₃ (337.37): C, 67.64; H, 5.68; N, 12.46; O, 14.22, Found: C, 67.61; H, 5.65; N, 12.42; O, 14.25.

5-(4-Hydroxyphenyl)-8,9-dihydropyrimido[4,5-*b*]quinoline-2,4,6(1H,3H,5H,7H,10H)-trione (4j)

Yield: 94%; white solid; mp >300 °C; FTIR (KBr) $\bar{\nu}$ (cm⁻¹): 3200 (NH), 2955 (C=C-H), 1691 (C=O), 1596 (C=C aromatic); ¹H NMR (DMSO-d₆, 400 MHz) δ (ppm): 1.01 (s, 6H, 2CH₃), 2.21 (s, 2H, CH₂), 2.49 (m, 2H, CH₂), 6.05 (s, 1H, CH), 6.95 (d, 2H, $J = 8$ Hz, H-Ar), 7.16 (d, 2H, $J = 8$ Hz, H-Ar), 7.43 (q, 2H, $J = 8$ Hz, H-Ar), 7.80 (s, 1H, OH), 7.94 (s, 1H, NH), 9.81 (s, 1H, NH), 10.32 (s, 1H, NH); Anal. Calcd. For C₁₉H₁₉N₃O₄: C, 64.58; H, 5.42; N, 11.89; O, 18.11, Found: C, 64.63; H, 5.36; N, 11.97; O, 18.04.

5-(4-Chlorophenyl)-8,8-dimethyl-7,8,9,10-tetrahydro-pyrimido[4,5-*b*]quinoline-2,4,6(1H,3H,5H)-trione (4 k)

Yield: 88%; white solid; mp > 300 °C; FTIR (KBr) $\bar{\nu}$ (cm⁻¹): 3142 (NH), 3055 (C=C-H), 1690 (C=O), 1595 (C=C aromatic); ¹H NMR (DMSO-d₆, 400 MHz) δ (ppm): 1.00 (s, 6H, 2CH₃), 2.06–2.21 (m, 4H, 2CH₂), 5.82 (s, 1H, NH), 6.95 (d, 2H, $J = 8$ Hz, H-Ar), 7.05–7.28 (m, 2H, H-Ar), 9.35 (s, 1H, NH), 9.81 (s, 1H, NH), 1.032 (s, 1H, NH); Anal. Calcd. For C₁₉H₁₈ClN₃O₃: C, 61.38; H, 4.88; N, 11.30, O, 12.92, Found: C, 61.42; H, 4.92; N, 11.25; O, 12.89.

5-(4-Nitrophenyl)-8,9-dihydropyrimido[4,5-*b*]quinoline-2,4,6(1H,3H,5H,7H,10H)-trione (4 l)

Yield: 92%; yellow solid; >300 °C; FTIR (KBr) $\bar{\nu}$ (cm⁻¹): 3370 (NH), 3135 (C=C-H), 1711 (C=O), 1652 (C=C aromatic), 1518, 1350(NO₂); ¹H NMR (DMSO-d₆, 400 MHz) δ (ppm): 1.80 (d, 2H, $J = 4$ Hz, CH₂), 2.21 (m, 2H, CH₂), 2.58 (d, 2H, $J = 4$ Hz, CH₂), 4.87 (s, 1H, CH), 7.34 (d, 2H, $J = 8$ Hz, Ar-H), 7.45(d, 2H, $J = 8.8$ Hz, Ar-H), 8.06 (d, 1H, $J = 8$ Hz, Ar-H), 9.03 (s, 1H, NH), 10.20 (s,

1H, NH), 10.60 (s, 1H, NH); Anal. Calcd. For C₁₇H₁₄N₄O₅: C, 57.63; H, 3.98; N, 15.81; O, 22.58, Found: C, 57.68; H, 4.09; N, 15.74; O, 22.49.

8,8-Dimethyl-5-phenyl-8,9-dihydro-1H-chromeno[2,3-d]pyrimidine-2,4,6(3H,5H,7H)-trione (C)

Yield: 95%; white solid; 161 °C^[49]; FTIR (KBr) $\bar{\nu}$ (cm⁻¹): 3478, 2936, 2864, 1683; ¹H NMR (DMSO-d₆, 400 MHz) δ (ppm): 0.96 (3H, s, CH₃), 1.13 (3H, s, CH₃), 2.11–2.57 (4H, m, 2CH₂), 4.56 (1H, s, CH), 7.16–7.23 (5H, m, H-Ar), 11.03 (1H, s, NH), 12.12 (1H, brs, NH).

4 | CONCLUSIONS

A green, facile, safe and eco-friendly protocol for the synthesis of dihydropyrimido[4,5-*b*]quinolinetriones in the presence of CoFe₂O₄@SiO₂/PPA under ultrasonic irradiation was presented. High efficient solid acid nanocatalyst, exhibited strong activity for the synthesis of mentioned products in excellent yields and short reaction times. The reaction conditions provided a green and facile pathway for the preparation of dihydropyrimido[4,5-*b*]quinolinetrione derivatives. Also, prepared solid acid catalyst can be considered as an excellent catalyst for use in other organic synthesis.

ACKNOWLEDGMENTS

Authors gratefully acknowledge the Chemistry Department of University of Kashan for supporting this work by grant number of 784946.

CONFLICT OF INTEREST

There are no conflicts to declare.

ORCID

Leila Moradi  <https://orcid.org/0000-0001-6830-907X>

REFERENCES

- [1] G. Cravotto, G. Palmisano, S. Tollari, G. M. Nano, A. Penoni, *Ultrason. Sonochem.* **2005**, *12*, 91.
- [2] K. Saïd, Y. Moussaoui, M. Kammoun, R. B. Salem, *Ultrason. Sonochem.* **2011**, *18*, 23.
- [3] J. Safaei-Ghomi, M. A. Ghasemzadeh, *J. Serb. Chem. Soc.* **2011**, *76*, 679.
- [4] A. C. Silva, A. L. F. de Souza, O. A. C. Antunes, *J. Organomet. Chem.* **2007**, *692*, 3104.
- [5] S. Rostamnia, L. Kamran, *Synthesis* **2011**, *11*, 3080.
- [6] S. Tangestaninejad, M. Moghadam, V. Mirkhani, H. Kargar, *Ultrason. Sonochem.* **2006**, *13*, 32.
- [7] M. Atobe, Y. Kado, R. Asami, T. Fuchigami, T. Nonaka, *Ultrason. Sonochem.* **2005**, *12*, 1.
- [8] A. M. A. Al-Kadasi, G. M. Nazeruddin, *J. Chem. Pharm. Res.* **2013**, *5*, 204.
- [9] G. V. Ambulgekar, B. M. Bhanage, S. D. Samant, *Tetrahedron Lett.* **2005**, *46*, 2483.
- [10] A. M. A. Al-Kadasi, G. M. Nazeruddin, *J. Chem. Pharm. Res.* **2010**, *2*, 536.
- [11] K. S. Suslick, *Science* **1990**, *247*, 1439.
- [12] K. S. Suslick, D. J. Flannigan, *Annual Rev. Phys. Chem.* **2008**, *59*, 659.
- [13] T. G. Leighton, *The Acoustic Bubble*, Academic Press, London **1994**.
- [14] K. S. Suslick, R. E. Cline Jr., D. A. Hammerton, *J. Am. Chem. Soc.* **1986**, *108*, 5641.
- [15] H. Z. He, Y. J. Jia, Q. G. Yao, S. J. Liu, H. K. Yue, H. W. Yu, R. S. Hu, *Ultrason. Sonochem.* **2015**, *22*, 144.
- [16] L. Moradi, M. Zare, *Green Chem. Lett. Rev.* **2018**, *11*, 197.
- [17] K. Rabiei, H. Naeimi, *Ultrason. Sonochem.* **2015**, *24*, 150.
- [18] B. Banerjee, *Ultrason. Sonochem.* **2017**, *35*, 15.
- [19] M. Nematpour, E. Rezaee, M. Jahani, S. A. Tabatabai, *Ultrason. Sonochem.* *50*, 1. <https://doi.org/10.1016/j.ultsonch.2018.08.001>
- [20] B. Banerjee, *Ultrason. Sonochem.* **2017**, *35*, 1.
- [21] A. Domling, I. Ugi, *Angew. Chem. Int. Ed.* **2000**, *39*, 3168.
- [22] I. Ugi, A. Domling, *Endeavour* **1994**, *18*, 115.
- [23] S. Heck, A. Domling, *Synlett* **2000**, 424.
- [24] D. J. Ramon, M. Yus, *Angew. Int. Ed.* **2005**, *44*, 1602.
- [25] R. Pontikis, C. Monneret, *Tetrahedron Lett.* **1994**, *35*, 4351.
- [26] D. Gandhi, S. Agarwal, *J. Heterocycl. Chem.* **2018**, *55*, 2977.
- [27] D. Gandhi, P. Kalal, P. Prajapat, D. K. Agarwal, S. Agarwal, *Comb. Chem. High Throughput Screening* **2018**, *21*, 236.
- [28] S. Agarwal, D. K. Agarwal, D. Gandhi, K. Goyal, P. Goyal, *Lett. Org. Chem.* **2018**, *15*, 863.
- [29] E. Lunt, in *Comprehensive Organic Chemistry*, (Eds: D. Barton, W. D. Ollis), Pergamon, Oxford **1974**.
- [30] J. D. Brown, in *Comprehensive Heterocyclic*, (Eds: K. A. R. Chemistry, C. W. Rees), Pergamon, Oxford **1984**.
- [31] T. K. Bradshaw, D. W. Hutchinson, *Chem. Soc. Rev.* **1977**, *6*, 43.
- [32] T. Miyasaka, H. Tanaka, M. Baba, H. Hayakawa, R. T. Walker, J. Balzarini, E. De Clercq, *J. Med. Chem.* **1989**, *32*, 2507.
- [33] R. E. Looper, M. T. C. Runnegar, R. M. Williams, *Angew. Chem. Int. Ed.* **2005**, *44*, 3879.
- [34] A. V. Zakharov, M. Y. Gavrilov, G. N. Novoselova, M. I. Vakhurin, M. E. Konshin, *Khim. Farm. Zh.* **1996**, *30*, 39.
- [35] A. Agarwal, R. Ashulosh, N. Goyal, P. M. S. Chauhan, S. Gupta, *Bioorg. Med. Chem.* **2005**, *13*, 6678.
- [36] E. M. Grivsky, S. Lee, C. W. Siggel, D. S. Duch, C. A. Nichol, *J. Med. Chem.* **1980**, *23*, 327.
- [37] A. B. Deyanov, R. K. Niyazov, F. Y. Nazmetdinov, B. Y. Syropyatov, V. E. Kolla, M. E. Konshin, *Khim. Farm. Zh.* **1991**, *25*, 26.
- [38] J. P. De la Cruz, T. Carrasco, G. Ortega, F. Sanchez De la Cuesta, *Lipid* **1992**, *27*, 192.

- [39] Y. S. Sanghhvi, S. B. Larson, S. S. Matsumoto, L. D. Nord, D. F. Smee, R. C. Willis, T. L. Avery, R. K. Robins, G. R. Revankar, *J. Med. Chem.* **1989**, 32, 629.
- [40] R. B. Tenser, A. Gaydos, K. A. Hay, *Antimicrob. Agents Chemother.* **2001**, 45, 3657.
- [41] K. Tabatabaeian, A. Fallah Shojaei, F. Shirini, S. Z. Hejazi, M. Rassa, *Chin. Chem. Lett.* **2014**, 25, 308.
- [42] A. Khalafi-Nejhad, A. Panahi, *Synthesis* **2011**, 6, 984.
- [43] D. Q. Shi, L. H. Niu, H. Yao, H. Jiang, *J. Het. Chem.* **2009**, 46, 237.
- [44] S. C. Jadhvar, H. M. Kasraliker, S. V. Goswami, S. R. Bhusare, *World J. Pharm. Pharm. Sci.* **2015**, 4, 1106.
- [45] B. P. Jacob, A. Kumar, R. P. Pant, S. Singh, E. M. Mohammed, *Bull. Mater. Sci.* **2011**, 34, 1345.
- [46] Z. Zi, Y. Sun, X. Zhu, Z. Yang, J. Dai, W. Song, *J. Magn. Magn. Mater.* **2009**, 321, 1251.
- [47] M. H. Mosslemin, M. R. Nateghi, *Ultrason. Sonochem.* **2010**, 17, 162.
- [48] K. Nikoofar, H. Heidari, Y. Shahedi, *Res. Chem. Intermed.* **2018**, 44, 4533.
- [49] R. Ghahremanzadeh, F. Fereshtehnejad, A. Bazgir, *Chem. Pharm. Bull.* **2010**, 58, 516.

SUPPORTING INFORMATION

Additional supporting information may be found online in the Supporting Information section at the end of the article.

How to cite this article: Moradi L, Mahdipour P. Green and rapid synthesis of dihydropyrimido [4,5-*b*]quinolinetrione derivatives using CoFe₂O₄@PPA as high efficient solid acidic catalyst under ultrasonic irradiation. *Appl Organometal Chem.* 2019;e4996. <https://doi.org/10.1002/aoc.4996>